Optik 159 (2018) 229–244

Contents lists available at ScienceDirect

Optik

journal homepage: www.elsevier.de/ijleo

Original research article

First principles investigation of optoelectronic properties of $ZnXP_2$ (X = Si, Ge) lattice matched with silicon for tandem solar cells applications using the mBJ exchange potential

Hamza Bennacer[a,b,*], Abdelkader Boukortt[b], Said Meskine[b], Moufdi Hadjab[c], Mohamed Issam Ziane[d], Ali Zaoui[e]

[a] University of M'sila, Faculty of Technology, 28000, M'sila, Algeria
[b] Elaboration and Characterization Physical Mechanics and Metallurgical of Material, Laboratory, ECP3M, Electrical Engineering Department, Faculty of Sciences and Technology, Abd elhamid Ibn Badis University, Mostaganem, 27000, Algeria
[c] Thin Films Development and Applications Unit UDCMA, Setif-Research Center in Industrial Technologies CRTI, Algiers, Algeria
[d] Research Center in Semi-conductor Technologies for Energetic (CRTSE), Division of Semi-conductors Crystalline Growth and Metallurgical Processes (CCPM/CSM), Algiers, Algeria
[e] Laboratoire de physique computationnelle des matériaux (LPCM), Université Djillali Liabès, Sidi Bel-Abbès, 22000, Algeria

ARTICLE INFO

Article history:
Received 29 December 2017
Accepted 21 January 2018

Keywords:
FP-LAPW
mBJ
Chalcopyrite
Electronic band structure
Linear optical properties

ABSTRACT

II-IV-V_2 materials are attractive compounds for optoelectronic, photonic and photovoltaic applications due to their valuable ternary chemistry. A primary technological challenge in photovoltaics is to find and develop a lattice matched efficient material to be used in combination with silicon for tandem solar cells. $ZnSiP_2$ and $ZnGeP_2$ chalcopyrites are promising semiconductors that could satisfy these criteria. Particularly, $ZnSiP_2$ is known to have bandgap energy of ~2 eV and a lattice mismatch with silicon of 0.5%. In this work, the first principle calculations have been performed to investigate the structural, electronic and optical properties of $ZnSiP_2$ and $ZnGeP_2$ in chalcopyrite structure within the Full Potential-Linearized Augmented Plane Wave (FP-LAPW) method based on the Density Functional Theory (DFT) as implemented in WIEN2K code. The local Density approximation (LDA) of Perdew and Wang was used as exchange-correlation potential to calculate the structural proprieties. Furthermore, the recently modified Becke-Johnson (mBJ) functional of Tran and Blaha was also employed to compute the electronic and optical properties in order to get best values of the band gap energy and some better degree of precision. The complex dielectric function, the complex refractive index, reflectivity, absorption coefficient, and the optical conductivity were calculated to illustrate the linear optical properties of both compounds $ZnSiP_2$ and $ZnGeP_2$. At last, the obtained results indicate that $ZnSiP_2$ and $ZnGeP_2$ are attractive materials in optoelectronic devices especially as a lattice matched material with silicon for tandem solar cells applications.

* Corresponding author at: University of M'sila, Faculty of Technology, 28000, M'sila, Algeria.
E-mail address: hamza.bennacer28@yahoo.fr (H. Bennacer).

https://doi.org/10.1016/j.ijleo.2018.01.079
0030-4026/

1. Introduction

Currently, the civilization and industries are extremely depending on energy. The ordinary resources of energy such as fossil oil and coal are limited by greenhouse gases as a byproduct [1]. Due to greenhouse gases, global warming is expected to increase, as humans add more greenhouse gases [1,2]. So, the solar energy appears to be the most promising to overcome these problems. As the sun is the most abundant, efficient and safe source of energy, photovoltaic solar cells are recently attracting special attention, but, the expensive costs and low efficiency of solar cells have limited their vast use in daily life [3]. However, new suitable materials for photovoltaic and solar cells fabrication technologies have become the object of investigation [3]. For solar cell application, the most important material requirement is that it possesses a high absorption coefficient and thereby should have an optimal direct band gap to absorb the visible light spectrum as well [3–6]. Among the candidate materials we find I-III-VI_2 and II-IV-V_2 chalcopyrites which, recently, have received much attention because of their potential applications in the field of light-emitting diodes, non-linear optical applications, and as a sensitive photovoltaic material in solar cells [7]. Several past studies, show that II-IV-V_2 compounds present higher properties compared to I-III-VI_2 chalcopyrites in terms of hardness, thermo-mechanical, thermo-optical, low scattering losses and non-linearity parameters [8–15]. II-IV-V_2 chalcopyrites are structural analogs to III-V semiconductors, where the group III element is substituted by alternating group II and group IV elements [16,17]. A large number of II-IV-V_2 compounds are formed from abundant and non-toxic elements making them attractive for photovoltaic applications [18]. A continual technological challenge in photovoltaic solar cells is the implementation of an optically lattice matched efficient material to be used in combination with silicon (Si) for tandem cells. $ZnSiP_2$ and $ZnGeP_2$ are among a few materials which are nearly lattice matched with Si and have appropriate band gaps for tandem dual-junction photovoltaics on Si [17]. $ZnSiP_2$ is considered as a promising compound with a band gap of 2.0 eV a lattice mismatch with Si of 5% [17–21]. We have noted that there have been various theoretical and experimental approaches to demonstrate and illustrate the different properties of $ZnSiP_2$ semiconductor [9,22–27]. Further, first principle calculations based on density functional theory (DFT) [28,29] have been used by several researchers to obtain the structural, electronic, optical and magnetic properties of II-IV-V_2 group of semiconductors [4,13,30–33]. Recently, $ZnGeP_2$ has been mainly studied for its capacity as nonlinear optical semiconductor [34]. However, through many years of research and study, there is still not an agreement about the nature of its band structure [34]. In addition, there have been several experimental and theoretical approaches [4,32,35–47] to explain the different physical properties of $ZnGeP_2$ semiconductor [48].

In this work, the structural, electronic and linear optical properties of the both chalcopyrite ternaries $ZnSiP_2$ and $ZnGeP_2$, have been studied, by using the full potential linearized augmented plane wave (FP-LAPW) method [49] based on density functional theory (DFT) [28,29,50]. As a first pace, we have studied the chalcopyrite structure and described the theoretical steps adopted to obtain the structural properties and total energies, where we have used a full total energy minimization for, firstly, obtaining the equilibrium c/a ratio and, secondly, we determined the equilibrium volume, bulk moduli and their derivative for this calculated c/a ratio. The electronic band structure, the density of states and the optical properties will also be computed and discussed in this paper.

2. Computational details

The present calculations are performed using the full-potential linearized augmented plane wave (FP-LAPW) method [51,52] as incorporated in Wien2k package [53].

We consider herein by II-IV-V_2 ternary compounds in body-centered tetragonal chalcopyrite structure (space group $I\bar{4}2d$), shown in Fig. 1, the lattice constant a corresponding to the lattice constant of a cubic zincblende structure, the c/a ratio, and the internal displacement parameter u revealing the distortion of the anion sublattice due to different surroundings. In the ideal structure, $c/a = 2$ and $u = 1/4$ [3,4,9].

Furthermore and in order to achieve energy eigenvalues convergence, the wave functions in the interstitial regions were expanded in plane wave with a cutoff R_{MT} x Kmax equal to 8, where R_{MT} is the minimum radius of the muffin-tin spheres and Kmax gives the magnitude of the largest k vector in the plane wave expansion. Inside the spheres, the valence wave functions were expanded up to $l_{max} = 10$. Intending to keep the same degree of convergence for all the lattice constants, we kept the values of the sphere radii and K_{max} constant over all the considered lattice spacing range. However, the smallest muffin-tin radius in the unit cell R_{MT}, was chosen for the expansion of the wave functions in the interstitial region while the charge density is Fourier expanded up to $G_{max} = 14$ $(Ryd)^{1/2}$. Hence, the muffin tin radii for Zn, Si, Ge and P are chosen to be 2.2, 2.0, 2.2 and 2.0 a.u, consecutively.

The exchange-correlation potential for structural properties was treated using only the local density approximation (LDA) of Perdew and Wang [54]. While for electronic properties, beside, the generalized gradient approximation of Perdew et al. (GGA PBEsol) [55] and the Engel–Vosko-GGA (EV-GGA) formalism [56] we have also applied the modified Becke-Johnson approach (TB-mBJ) proposed recently by Tran and Blaha [57,58] to optimize the corresponding potential for calculating the band structure [59]. The latter has proven to be a promising tool for accurate determination of the fundamental band gaps of wide-band-gap insulators, semiconductors, transition-metal oxides [57,60], half-metallicity [61,62], and doped semiconductors systems [4,57,58,63–66]. Regarding the extraction of optical properties, we also employed the modified Becke-Johnson

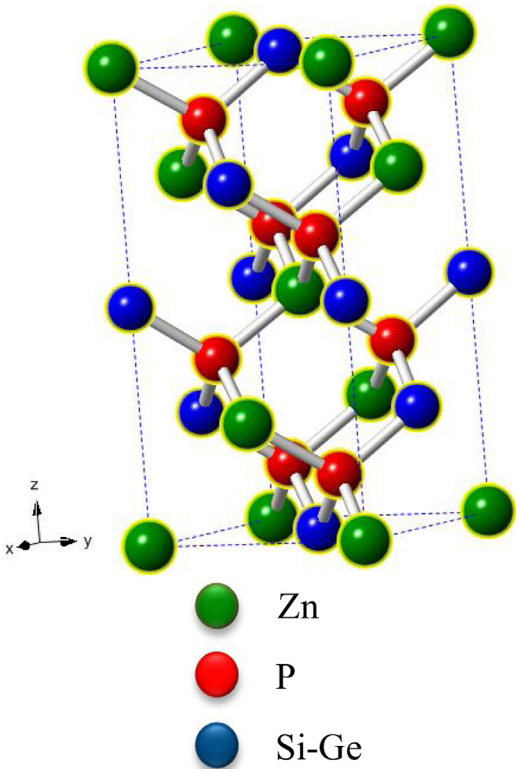

Fig. 1. The crystal structure of chalcopyrite $ZnXP_2$ (X = Si, Ge) compounds.

scheme (mBJ). This method is a modified version of the Becke-Johnson potential that had been used to improve band gaps obtained by ordinary and conventional DFT-based methods. The mBJ potential can be written as:

$$\upsilon_{x,\sigma}^{mBJ}\left(\vec{r}\right) + (3c-2)\frac{1}{\pi}\sqrt{\frac{5}{6}\sqrt{\frac{\tau_\sigma\left(\vec{r}\right)}{\rho_\sigma\left(\vec{r}\right)}}} \tag{1}$$

where ρ_σ is the electron density, τ_σ is the kinetic-energy and $\upsilon_{x,\sigma}^{mBJ}$ is the Becke-Roussel potential [67]. The c parameter is a system dependent parameter, with c equal to 1 corresponding to the original Becke-Johnson potential. For Bulk crystalline materials, Tran and Blaha proposed to determine c by the following empirical relation:

$$c = \alpha + \beta\left(\frac{1}{V_{cell}}\int_{cell}\frac{\left|\nabla\rho_\sigma(r')\right|}{\rho_\sigma(r')}d^3r'\right)^{\frac{1}{2}} \tag{2}$$

where V_{cell} represents the unit cell volume, $\alpha = -0.012$ and $\beta = 1.023$ bohr$^{1/2}$ are fitted parameters according to experimental values [57,68].

The self-consistent calculations are considered to be converged when the total energy of the system is stable [69,70] within 10^{-4} Ryd. The integrals over the Brillouin zone are performed up to 102 k-points, (grid of 10_10_10 meshes, and equivalent to 1000 k-points in the entire Brillouin zone).

In the optical properties calculations we used the equivalent to 20,000 k-points in the entire Brillouin zone by the OPTIC code [71], as implemented in the all-electron WIEN2K method [53]. It has been shown by Del Sole and Girlanda [72], TB-mBJ is combined with the scissor-operator approximation to describe the optical spectrum rather accurately. We have therefore made a correction ΔEg to the gaps. The corrections to the FP-LAPW band gaps are $\Delta Eg = 0.21$ eV for $ZnSiP_2$ and $\Delta Eg = 0.52$ eV for $ZnGeP_2$.

Table 1
Calculated structural properties: lattice parameter *a*, *c*, internal parameter *u*, bulk modulus *B*, its pressure derivative *B'*, the lattice mismatching to Si $\Delta a/a$ and the enthalpy of formation $\Delta_f H$ according to LDA approximation for both ternaries $ZnSiP_2$ and $ZnGeP_2$ in the chalcopyrite structure, in comparison with Si and other experimental data and theoretical calculations.

		a (Å)	c(Å)	c/a	*u*	B(GPa)	B'	Lattice mismatching to Si (%)	Δ_fH (T = 0 K) (RyD)
$ZnSiP_2$	LDA	5.407	10.451	1.93	0.264	100.360	4.979	0.440	−5530.664
	Exp	5.399[a,b]	10.435[a,b]	1.932[a,b]	0.269[a,b]				
		5.425[c]	10.552[c]	1.94[c]	0.269[c]				
		5.407[d]	10.451[d]	1.930[d]					
		5.400[e]	10.436[e]	1.932[e]					
		5.401[f]	10.443[f]						
		5.399[a]	10.436[a]	1.933[a]	0.271[a]				
	Exp							0.500[g]	
$ZnGeP_2$	LDA	5.406	10.596	1.96	0.250	89.873	4.667	0.460	−9144.817
		5.466[h]	10.722[h]	1.961[h]					
		5.502[c]	10.850[c]	1.972[c]	0.254[c]				
	Exp	5.46[a]	10.710[a]	1.960[a]	0.258[a]				
		5.465[i]	10.766[i]	1.970[i]	0.250[i]				
		5.480[j]	10.795[j]	–	0.254[j]				
		5.473[f]	10.717[f]						
	Exp	5.463[k]	10.734[k]	1.965[k]	0.258[k,l]				
	Exp				0.267[a]				
Si	Exp	5.431[m]							

[a] Ref. [13].
[b] Ref. [74].
[c] Ref. [4].
[d] Ref. [75].
[e] Ref. [76].
[f] Ref. [77].
[g] Ref. [17].
[h] Ref. [14].
[i] Ref. [10].
[j] Ref. [78].
[k] Ref. [34].
[l] Ref. [79].
[m] Ref. [80].

3. Results and discussion

3.1. Geometry and structure optimization

The ternary $ZnXP_2$ (X = Si, Ge) compounds crystallize in the chalcopyrite structure with space group $I\bar{4}2d$ (no. 122), are shown in Fig. 1. It has been observed that the structure of those compounds is rather similar to that of the ideal twice zinc-blende cell characterized by its rapport c/a = 2 and its internal structural parameter μ = 0.25, which describe the position of (P) atom. In order to gain deep insight into the equilibrium structural properties, we have performed volume optimization; hence the calculated total energy as a function of the volume was used for determination of equilibrium lattice constant, bulk modulus and its pressure derivative, through fitting the total energy versus volume to Murnaghan's equation of states (EOS) [73]. The optimized structural values are listed in Table 1 alongside with the experimental and other theoretical results [4,10,13,14,17,34,74–80]. We present the calculated lattice constants (a, c), the internal structural parameters u, the bulk modulus B and its first derivative B′ of $ZnSiP_2$ and $ZnGeP_2$, the lattice mismatch with silicon Si(Δa/a) and the enthalpy energy of formation Δ_fH using LDA approximation. As it could be seen from Table 1, the computed lattice constants for $ZnSiP_2$ and $ZnGeP_2$ are found to be in reasonable agreement with those obtained by experimentation end other calculations. In the case of the bulk modulus, our calculations predict the values of 100.36 and 89.87 GPa for $ZnSiP_2$ and $ZnGeP_2$ respectively. Compared to the other data shown under Table 1, we may conclude that LDA leads to underestimating our calculated values which are found to be in agreement with the previous data. We also noticed a small mismatch (less than 0.5%) between the two compounds $ZnXP_2$ (X = Si, Ge) and silicon. The computed and experimental lattice constants of $ZnXP_2$ (X = Si, Ge) matched to Si are plotted in Fig. 2. This result allows us to assume that $ZnSiP_2$ and $ZnGeP_2$ are suitable for silicon substrates. The lattice mismatch is given by [81,82]:

$$\frac{\Delta a}{a_{Si}} = \frac{a_{ZnXP_2} - a_{Si}}{a_{Si}} 100\% \tag{3}$$

The enthalpy of formation, Δ_fH (Rydberg unit of energy), of $ZnSiP_2$ and $ZnGeP_2$ at zero temperature and pressure (0K and 0P) is calculated according to the following relations [83,84]:

$$\Delta_f H(ZnSiP_2) = E^{\min}_{ZnSiP_2} - \left[E^{\min}_{Zn} - E^{\min}_{Si} - 2E^{\min}_{P}\right] \tag{4}$$

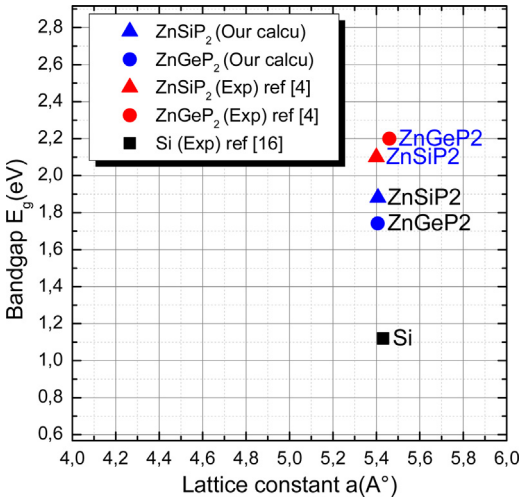

Fig. 2. Band gaps and lattice constants for $ZnSiP_2$ and $ZnGeP_2$ in comparison with Si.

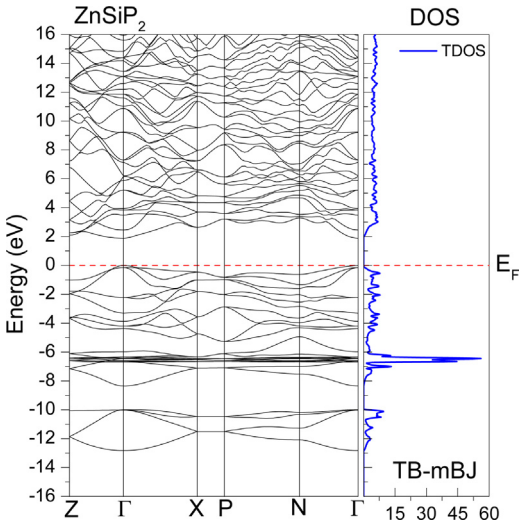

Fig. 3. Calculated band structure and total density of state for $ZnSiP_2$ with mBJ approximation.

$$\Delta_f H(ZnGeP_2) = E^{\min}_{ZnGeP_2} - \left[E^{\min}_{Zn} - E^{\min}_{Ge} - 2E^{\min}_{P}\right] \quad (5)$$

where $E^{\min}_{ZnSiP_2}$ and $E^{\min}_{ZnGeP_2}$ are the total minimum energies of the $ZnSiP_2$ and $ZnGeP_2$, respectively. $E^{\min}_{Zn}$, $E^{\min}_{Si}$, $E^{\min}_{Ge}$ and $E^{\min}_{P}$ are the pure total minimum energies of Zn, Si, Ge and P, successively. Our calculations show that the enthalpy of formation becomes bigger when we changed Si element by Ge.

3.2. Electronic properties

In this section, we have calculated and plotted the electronic properties of $ZnSiP_2$ and $ZnGeP_2$ in the chalcopyrite structure at the equilibrium lattice constants by using the GGA PBEsol, EV-GGA and TB-mBJ approximations. We have found an important similarity behavior between the results obtained with the three approximations used in our work. Therefore, we have preferred to discuss only the results within TB-mBJ. The obtained band structures and the total densities of state (TDOS) with TB-mBJ are shown in Figs. 3 and 4 for $ZnSiP_2$ and $ZnGeP_2$, respectively.

As for Table 2, it presents our gap energy values for both compounds $ZnSiP_2$ and $ZnGeP_2$ calculated with GGA-PBESol, EV-GGA and mBJ approximations, which agree well, compared with other theoretical and experimental values [4,14,75,80,85]. The TB-mBJ calculations show that $ZnSiP_2$ and $ZnGeP_2$ are semiconductors with direct and indirect energy gap, successively. In the case of $ZnSiP_2$, the valence band maximum (VBM) and the conduction band minimum (CBM) are located at Γ point, resulting in a direct energy gap of 1.881 eV. Whereas concerning $ZnGeP_2$, the valence band maximum (VBM) and the conduction band minimum (CBM) are located at Γ and Z, consecutively, resulting indirect gap of 1.742 eV. In addition to this,

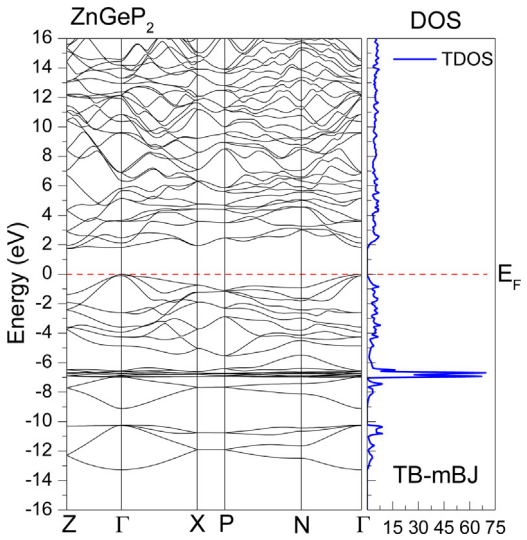

Fig. 4. Calculated band structure and total density of state for $ZnGeP_2$ with mBJ approximation.

Table 2
The calculated values of band gap energy of both compounds $ZnSiP_2$ and $ZnGeP_2$ obtained within mBJ approximation in comparison with Si and other experimental data and theoretical values.

Material		*Eg (eV)*			
	Our work GGAPBEsol	Our work EV-GGA	Our work TB-mBJ	Other theoretical works	Exp.
$ZnSiP_2$	1.138 (d)	1.257 (d)	1.881 (d)	1.98[a], 1.81[b]	2.0–2.3[a], 2.3[c],2.96[b]
$ZnGeP_2$	1.061 (i)	1.155 (i)	1.742 (i)	1.82[a],	1.8–2.2[a], 2.34[c,b] (d), 2.2[d]
	1.136 (d)	1.261 (d)	1.823 (d)	1.19[b](d)	
Si					1.12[e] (i)

[a] Ref. [4].
[b] Ref. [14].
[c] Ref. [75].
[d] Ref. [85].
[e] Ref. [80].

the direct band gap (Γ–Γ) shown in Fig. 4 of $ZnGeP_2$ indicate a value of 1.823 eV. It is clear that TB-mBJ approach gives better values of the band gap energy, which agree perfectly with the experiment and other theoretical calculation.

The energy distributions of different electronic states can be elucidated and explained via computing the density of states (DOS). The total densities of states (TDOS) along with the partial densities of state (PDOS) have been calculated for those compounds within mBJ method, as displayed in Fig. 5 for the $ZnSiP_2$ and Fig. 6 for the $ZnSiP_2$. A dashed vertical line shows the position of Fermi level (E_F).

From Figs. 3 and 5, we should emphasize that there are two distinct band structures in the density of electronic states in the $ZnSiP_2$ in the valence band region. The lowest band is in the energy range between −12.83 and −9.82 eV originates from P_s states. The second region band is located between −8.34 eV and Fermi energy (E_F) that is itself divided in two sub-bands, the first ranging from −8.34 and −6 eV which is, mainly, Zn_d states, while the second formed with significant contributions from Si_p and P_p states. The conduction band ranging from 1.88 to 16.0 eV is principally composed of a mixture of Si/P_ p, d states.

On the other side and according to Figs. 4 and 6, there are three distinct structures in the density of electronic states for the $ZnGeP_2$ separated by a gap. The lowest structure in the energy range between −13.28 and −10.19 eV originates from P_s states. The second region band is located between −9.08 eV and Fermi energy (E_F) that is itself divided onto two sub-bands: the first ranging from −9.08 to −5.64 eV which is, mainly, Zn_d states, while the second is formed of significant contributions from Ge/P_p states. The conduction band, the group ranging from 1.74 to 16.0 eV is originally composed of Ge/P_ p, d states.

3.3. Optical properties

After having defined the structural and electronic properties, we focus our study and discussion, on the linear optical properties of these materials, which are considered as a potential source of information concerning the electronic bands structures. Accordingly, in this part, the dielectric function, the refractive index, the reflectivity, the absorption coefficient and the optical conductivity of the ternaries $ZnSiP_2$ and $ZnGeP_2$ have been calculated and plotted within TB-mBJ approximation in

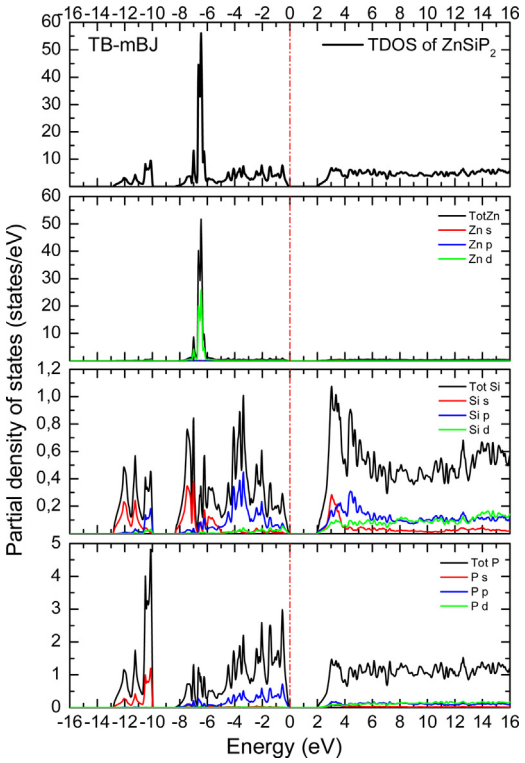

Fig. 5. Partial densities of states of $ZnSiP_2$ with mBJ approximation.

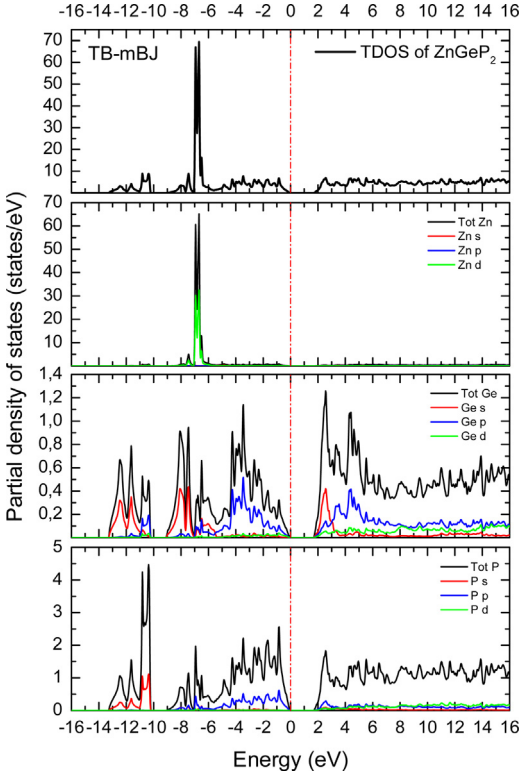

Fig. 6. Partial densities of states of $ZnGeP_2$ with mBJ approximation.

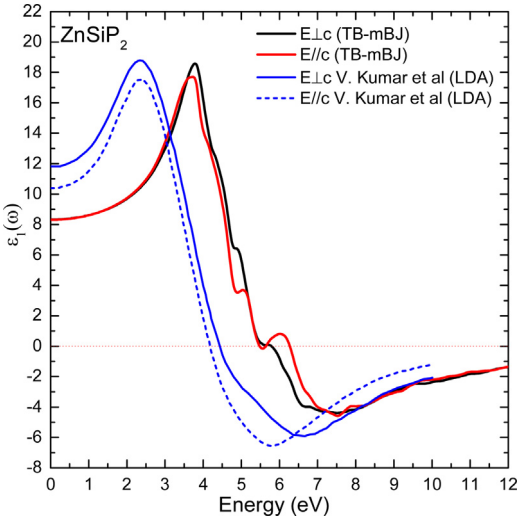

Fig. 7. Real part of the dielectric function for $ZnSiP_2$ within modified Becke-Johnson approximation (mBJ) compared with other computational work [22].

both crystallographic directions of polarization, ordinary (E//c axis) and extraordinary ($E \perp c$axis) [3]. As for scissor energy, the values of 0.210 eV and 0.520 eV for the $ZnSiP_2$ and $ZnGeP_2$ consecutively have been used. The optical properties are usually deduced from the complex dielectric function $\varepsilon(\omega)$ that is given by the following expression [80,86,87]:

$$\varepsilon(\omega) = \varepsilon_1(\omega) + i\varepsilon_2(\omega) \tag{6}$$

wherein, $\varepsilon_1(\omega)$ and $\varepsilon_2(\omega)$ are the real and imaginary parts of the complex dielectric function, respectively, and ω is the angular frequency. In the presence of electric field$\vec{E}$, the frequency dependent dielectric function is disjoined into parts: the interband and the intraband transitions. The information related to the interband transitions is exploitable for the semiconductors, while, the intraband for metals. The interband transitions are furthermore divided into direct and indirect bands transitions. The indirect band transition has a negligible contribution to $\varepsilon(\omega)$, which involves electron phonon scattering [48]. Whereas, the direct band contribution to the imaginary part of the dielectric function can be calculated from the momentum matrix elements between occupied and unoccupied wave functions [22,48].

To set frequency dependent dielectric function $\varepsilon(\omega)$, we need energy eigenvalues and electron wave functions, which are mutually considered as the natural output for band structure calculation [3,87]. Nevertheless, the dielectric function imaginary part $\varepsilon_2(\omega)$ is obtained from the joint density of state as well as from the momentum matrix elements. The real part is then derived from the imaginary part by imposing the Kramer-Kronig relation [3,8,68,82,86]. From the two components of the dielectric function $\varepsilon_1(\omega)$ and $\varepsilon_2(\omega)$, we can deduce the other optical quantities such as refractive index n(ω), extinction coefficient k(ω), absorption coefficient α(ω), reflectivity R(ω), and optical conductivity σ(ω) [3,68].

3.3.1. Dielectric function

This function can be calculated based on the band-structure results. The obtained TB-mBJ results of the real part $\varepsilon_1(\omega)$for $ZnSiP_2$ and $ZnGeP_2$ are shown in Figs. 7 and 8, respectively, compared to previous theoretical works [22,48]. For $ZnSiP_2$, $\varepsilon_1(\omega)$is positive up to 5.78 and 6.27 eV, consecutively, for $\varepsilon_1^{xx}(\omega)and\varepsilon_1^{zz}(\omega)$. After that, $\varepsilon_1(\omega)$ becomes negative and takes a minimum value, then, increases towards zero at higher energies level slowly. The plots shown in Fig. 7, present several peaks located at 3.79, 4.85, and 5.70 eV for the $\varepsilon_1^{xx}(\omega)$while at 3.74, 5.04 and 6.00 eV concerning $\varepsilon_1^{zz}(\omega)$. It is also positive for $ZnGeP_2$. It reaches 6.05 and 6.29 eV for$\varepsilon_1^{xx}(\omega)$ and$\varepsilon_1^{zz}(\omega)$, successively, and has peaked five peaks at 3.35, 4.14, 4.47, 4.85, and 5.94 eV regarding$\varepsilon_1^{xx}(\omega)$. Other peaks have been noticed, as for $\varepsilon_1^{zz}(\omega)$, which indicate 3.27, 3.85, 4.25, 5.45, and 6.29 eV. After this energy range, $\varepsilon_1(\omega)$ becomes negative and gets a minimum value. But it slowly, increases towards zero at higher energies level. Furthermore, the obtained values of static dielectric constant $\varepsilon_1(0)$ for $ZnSiP_2$ and $ZnGeP_2$ are listed in Table 2 compared with other theoretical data [46], where, the static constants of $ZnSiP_2$ are found to be 8.32 and 8.30 eV, respectively, for$\varepsilon_1^{xx}(0)$ and $\varepsilon_1^{zz}(0)$. In the opposite, the static constants are localized at 8.53 eV for $\varepsilon_1^{xx}(0)$ and 8.55 eV for $\varepsilon_1^{zz}(0)$when concerning $ZnGeP_2$.

The imaginary part of dielectric function is a necessary amount. It indicates the difference interband transitions in the semiconductor [3,87]. Our calculated imaginary part $\varepsilon_2(\omega)$ for $ZnSiP_2$ shown in Fig. 9, compared to other calculation data [46], display six sharp peaks at about 2.09, 2.77, 3.94, 4.64, 5.24, and 6.35 eV for$\varepsilon_2^{xx}(\omega)$. They are parallel to $\varepsilon_2^{zz}(\omega)$ peaks: 2.09, 2.84, 4.17, 4.66, 5.09, and 5.99 eV. From their part, the both calculated $\varepsilon_2^{xx}(\omega)$ and $\varepsilon_2^{zz}(\omega)$curves of $ZnGeP_2$ in Fig. 10, compared to other theoretical data [46,48], show a sharp increase at about 2.26 eV, at the first onset E_0 of the direct optical transitions. While, the first main peak is approximate to 2.95 eV in the ordinary direction (E⊥c) and 2.88 eV in the extraordinary direction (E//c), the second one draws near 3.69 and 3.58 eV for ordinary and extraordinary direction consecutively. Concerning the

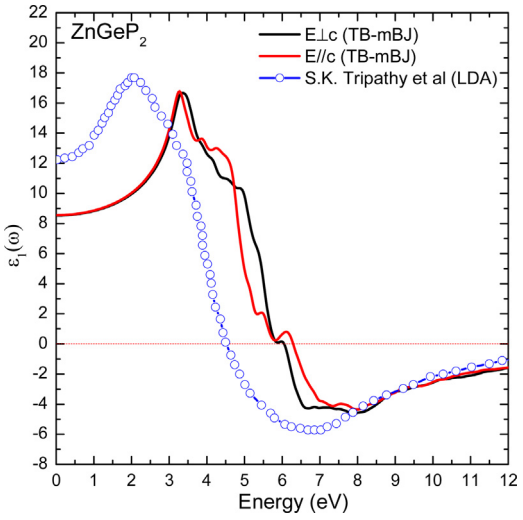

Fig. 8. Real part of the dielectric function for $ZnGeP_2$ within modified Becke-Johnson approximation (mBJ) compared with other computational work [48].

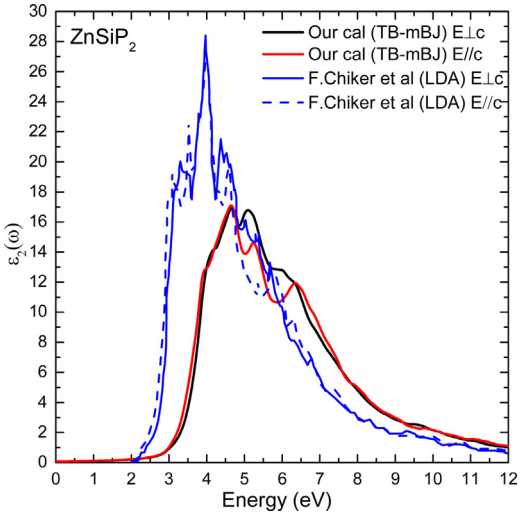

Fig. 9. The computed imaginary part of the dielectric function of $ZnSiP_2$ by using mBJ approach compared with other computational work [46].

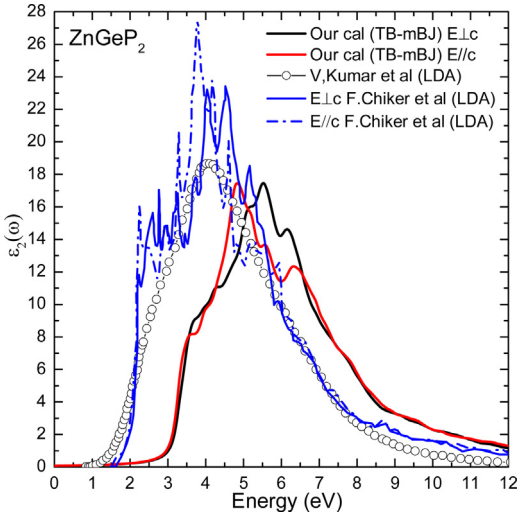

Fig. 10. The computed imaginary part of the dielectric function of $ZnGeP_2$ by using mBJ approach compared with other computational work [22,46].

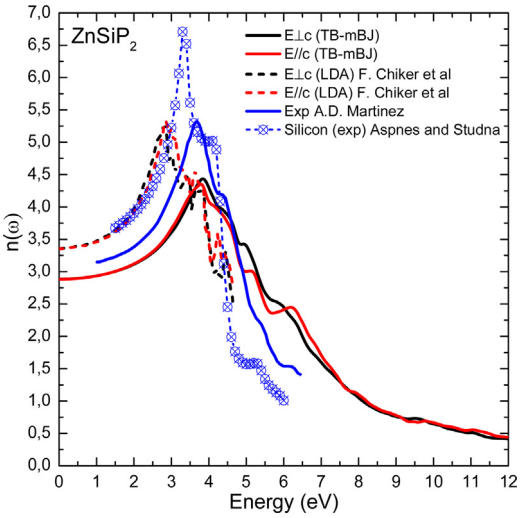

Fig. 11. The calculated refractive index of $ZnSiP_2$ within mBJ approximation compared to Si [90], experimental [17] and other computational data [46].

Table 3
The calculations values of static optical parameters $\varepsilon_1(\omega)$, $n(\omega)$ and $R(\omega)$ compared with other calculations values.

		$\varepsilon_1(0)$	n(0)	R(0)
$ZnSiP_2$	$E \perp c$	8.321	2.885	0.235
	$E \| c$	8.308	2.882	0.235
$ZnGeP_2$	$E \perp c$	8.530	2.921	0.240
	$E \| c$	8.550	2.925	0.240
		12.230[a]		
	$E \perp c$	12.524[b]		
	$E \| c$	12.805[b]		

[a] Ref. [22].
[b] Ref. [46].

third, the fourth, and the fifth they are located at 4.26, 5.54, and 6.15 eV for ordinary direction (E⊥c), whereas, 4.01, 4.81, and 6.31 eV relating to extraordinary direction (E//c). A wide values of imaginary part $\varepsilon_2(\omega)$ indicated in Figs. 9 and 10, means a large absorption of $ZnSiP_2$ and $ZnGeP_2$.

3.3.2. *Refractive and extinctive indexes*

The complex index of refraction can be calculated from the following expression [3,86,88]:

$$n(\omega) + ik(\omega) = \sqrt{\varepsilon_1(\omega) + i\varepsilon_2(\omega)} \tag{7}$$

Where the refractive index $n(\omega)$ and the extinction coefficient $k(\omega)$ can be computed from the next equations [3,86,88]:

$$n(\omega) = (1/\sqrt{2})\left[\sqrt{\varepsilon_1(\omega)^2 + \varepsilon_2(\omega)^2} + \varepsilon_1(\omega)^2\right] \tag{8}$$

$$k(\omega) = (1/\sqrt{2})\left[\sqrt{\varepsilon_1(\omega)^2 + \varepsilon_2(\omega)^2} - \varepsilon_1(\omega)^2\right] \tag{9}$$

The refractive index $n(\omega)$ is an essential physical parameter allied to the microscopic atomic interactions. Its values are often required to elucidate various types of spectroscopic data [3,86]. This parameter has a fundamental impact in optical properties for optoelectronic, photonic and photovoltaic devices. Actually, this optical parameter can measures the transparency of materials versus spectral radiations [89]. Any semiconductor refractive index $n(\omega)$ is computed through the real dielectric function [3,87]:

$$n = \sqrt{\varepsilon_1} \tag{10}$$

On Figs. 11 and 12, we have presented the calculated spectral plots of the refractive index for the pair of compounds $ZnSiP_2$ and $ZnGeP_2$, in series, using TB-mBJ approach compared with other available experimental and theoretical data [8,17] at the same time with the experimental refractive index of Silicon [90], over a range of photon energies up to 12 eV. The calculated static components of refractive index (zero refractive index $n(0) = \sqrt{\varepsilon_1(0)}$) for both ternaries are presented in Table 3. So, the static refractive index for low frequency, related to the ternaries $ZnSiP_2$ and $ZnGeP_2$, respectively, having the values of 2.885 and 2.921 concerning the ordinary direction $n(\omega)\perp$, while 2.882 and 2.925 regarding to the extraordinary direction $n(\omega)\|$.

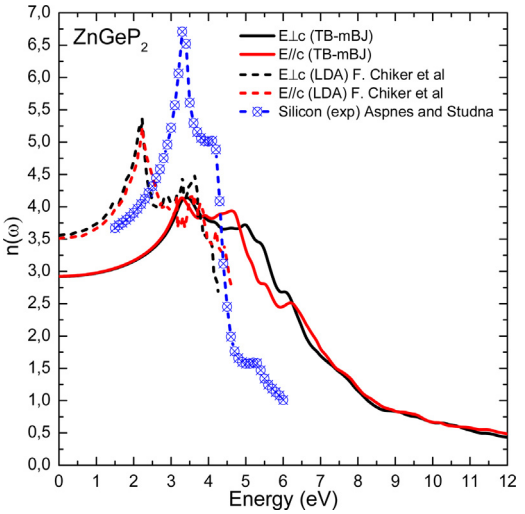

Fig. 12. The calculated refractive index of $ZnGeP_2$ within mBJ approximation compared to Si [90] and other computational data [46].

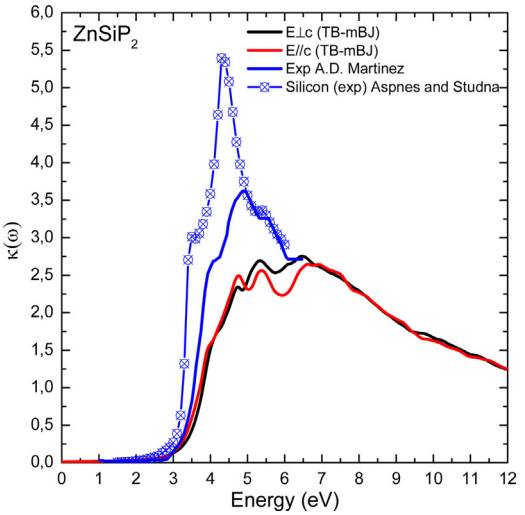

Fig. 13. Extinction coefficient of $ZnSiP_2$ within mBJ approximation compared to Si [90] and other experimental work [17].

The curves displayed in Figs. 11 and 12, indicate a maximum value at 3.85 and 3.79 eV following $n(\omega)\perp$, Meanwhile, 3.42 and 3.28 eV as for $n(\omega)\|$, for both compounds $ZnSiP_2$ and $ZnGeP_2$. It is obvious that the two components $n(\omega)\perp$ and $n(\omega)\|$ show weak isotropy at different energies range (0–12) eV. For $ZnSiP_2$ or $ZnGeP_2$, the $n(\omega)$ reaches a maximum value in the near ultraviolet (UV-A) light region.

Moreover, the calculated extinction coefficient $k(\omega)$ within TB-mBJ scheme for the two compounds $ZnSiP_2$ and $ZnGeP_2$ compared to Si, are given in Figs. 13 and 14, consecutively. The extinction coefficient of $ZnSiP_2$ shown in Fig. 13 compared with the experimental work of Martinez et al. [17], indicates maximum values at 2.75 and 2.64 for $k^{xx}(\omega)$and$k^{zz}(\omega)$. Furthermore, the plots $k^{xx}(\omega)$and$k^{zz}(\omega)$in Fig. 14 show maximum values at about 2.90 and 2.65, sequentially. We distinguish a several peaks resulting from the shift of electrons from the valence band to the conduction one.

3.3.3. *Absorption coefficient*

The optical absorption coefficient $\alpha(\omega)$ is one of the most crucial evaluation criteria for the optoelectronic materials, in photovoltaics [3,91–93] especially. The phenomenon of the absorption is generated when the photon energy of the incident beam is greater than the energy band gap [89]. The absorption coefficient $\alpha(\omega)$ is determined by the expression:

$$\alpha(\omega) = (4\pi/\lambda)k(\omega) \tag{11}$$

Our calculated absorption coefficient spectra $\alpha(\omega)$ for the herein investigated compounds within TB-mBJ approximation compared with other theoretical and experimental works [17,22,48,94,95,96] as shown in Figs. 15 and 16, display that these

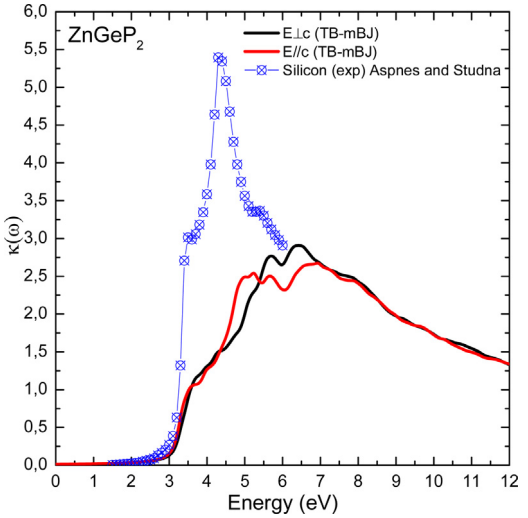

Fig. 14. Extinction coefficient of $ZnGeP_2$ within mBJ approximation compared to Si [90].

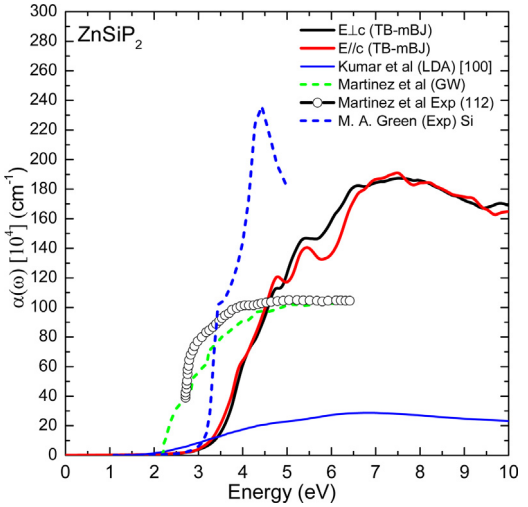

Fig. 15. Absorption coefficient of $ZnSiP_2$ within mBJ approach in comparison with Si [96] and other experimental and computational data [17,22].

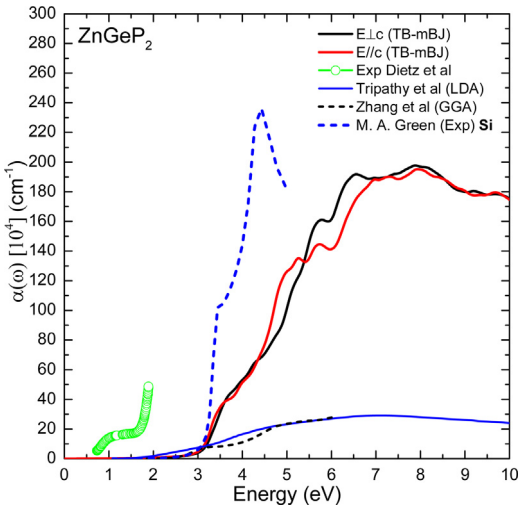

Fig. 16. Absorption coefficient of $ZnGeP_2$ within mBJ approach in comparison with Si [96] and other experimental and computational data [48,94,95].

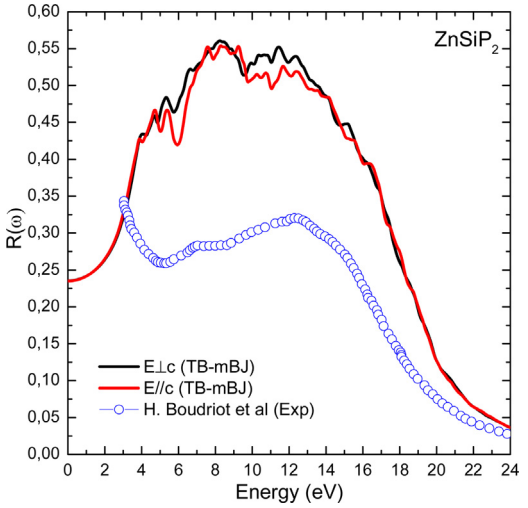

Fig. 17. Reflectivity of $ZnSiP_2$ within mBJ approach compared with experimental work of H. Boudriot et al. [98].

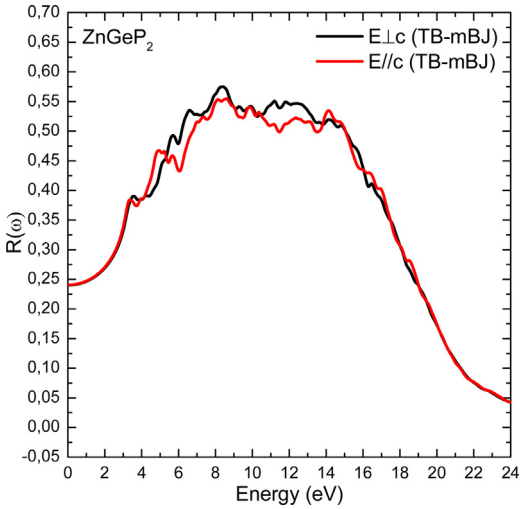

Fig. 18. Reflectivity of $ZnGeP_2$ within mBJ approach.

materials have a high optical absorption in a wide energy range of 2.09–7.50 eV and 2.26–7.93 eV, which corresponds to wave length range of (165–600) nm and (156–550) nm for the $ZnSiP_2$ and $ZnGeP_2$ in order of appearance.

From the features of the absorption coefficient spectra (Figs. 15 and 16), the absorption edges of $ZnSiP_2$ and $ZnGeP_2$ are located at 2.09 and 2.26 eV, respectively. It is concluding that both $ZnSiP_2$ and $ZnGeP_2$ are promising materials in solar cells application.

3.3.4. *Reflectivity*

Reflectivity of light R(ω) is one of the important parameters in linear optical calculations for many devices and applications such as solar cells. Furthermore, reflectivity depends on both parts of the complex refraction index n and k [68,89,97] which can be obtained from Eq. (10) [97].

$$R(\omega) = \frac{(n(\omega)-1)^2 + k(\omega)^2}{(n(\omega)+1)^2 + k(\omega)^2} \tag{12}$$

The computed reflectivity spectra for $ZnSiP_2$ and $ZnGeP_2$ by using TB-mBJ functional are illustrated in Figs. 17 and 18, in order, for different photonic energies. The zero frequency reflectivity R(0) of the investigated materials are listed in Table 3. The maximum values of $R_{xx}(\omega)$and$R_{zz}(\omega)$, respectively, are positioned at 8.23 and 8.28 eV for $ZnSiP_2$, whilst, 8.42 and 8.58 eV values are concerned with $ZnGeP_2$.

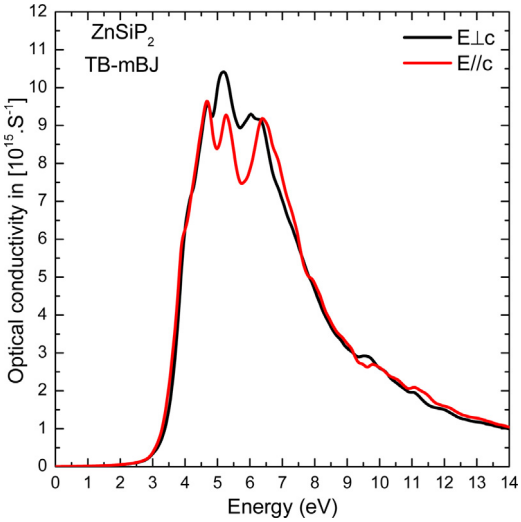

Fig. 19. Optical conductivity for $ZnSiP_2$ compound within modified Becke-Jonson approach.

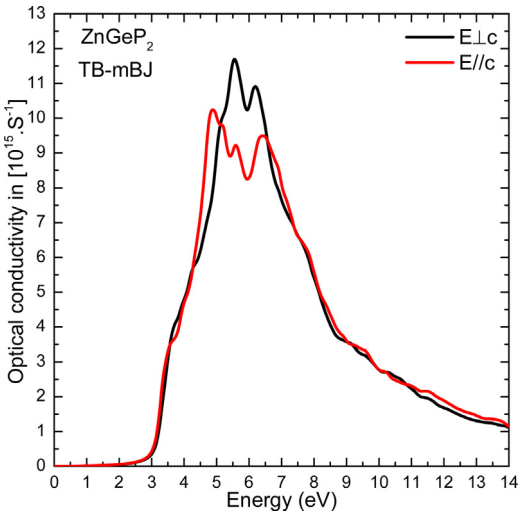

Fig. 20. Optical conductivity for $ZnGeP_2$ compound within modified Becke-Jonson approach.

Table 4
The different peaks and their width of the optical conductivity for $ZnSiP_2$ and $ZnGeP_2$ calculated within mBJ approach.

Compounds		$ZnSiP_2$	$ZnGeP_2$
Peak	$E \perp c$	5.183 eV	5.510 eV
	$E \parallel c$	4.671 eV	4.857 eV
Width	$E \perp c$	6.203 eV	5.665 eV
	$E \parallel c$	6.203 eV	5.892 eV

3.3.5. *Optical Conductivity*

The optical conductivity σ(ω) is deduced from the dielectric function which is given by [3]:

$$\sigma(\omega) = -(i\omega/4\pi)\varepsilon(\omega) \tag{13}$$

The curves of the optical conductivity σ(ω) calculated within TB-mBJ approximation are displayed in Figs. 19 and 20 over the range of photon energy up to 14 eV, for ternaries $ZnSiP_2$ then $ZnGeP_2$. Several critical peaks are presented in the feature of σ(ω) curves (see Figs. 19 and 20), which vary in conformity with the energy band gap and are corresponding with the bulk Plasmon excitations caused by electrons crossing from the valence to the conduction band [3]. The positions of the main peak and the total widths of the optical conductivity for both compounds $ZnSiP_2$ and $ZnGeP_2$ are presented in Table 4.

4. Conclusion

In this investigation study, we have used the ab-initio calculations, applying the all-electron FP-LAPW method of DFT within LDA approximation and mBJ exchange potential to estimate the structural and the optoelectronic properties, respectively, in the aim to assess the feasibility of $ZnSiP_2$/Si and $ZnGeP_2$/Si tandem solar cells. Initially, we have predicted the structural properties of both compounds by using LDA scheme. The obtained results show good agreement with experimental and other theoretical data. We have confirmed that both $ZnSiP_2$ and $ZnGeP_2$ are semiconductors. Moreover, the present calculation within mBJ approach indicates a direct band gap for $ZnSiP_2$. Whereas, the $ZnGeP_2$ band gap is founded as indirect one. Our calculated band gaps are in good harmony with the experimental and reported values. Based on this matching agreement, the linear optical properties were calculated and discussed in details for both polarizations ($E\perp c$ and $E//c$). The obtained results indicate that our studied ternaries offer an expanded phase for enhanced optoelectronic devices and solar cell applications. Finally, we have concluded that our estimated band gaps, absorption coefficient and reflectivity make both materials suitable and have a particular interest for a $ZnSiP_2$/Si and $ZnGeP_2$/Si tandem solar cell application.

Acknowledgments

The author is deeply grateful to all collaborators who participated in this work. Also, we are grateful to Mr. Benaissa Sid Ali (M'sila University, Algeria) for their valuable and useful discussions.

References

[1] Bhuiyan, et al., IEEE J. Photovolt. 2 (July (3)) (2012).
[2] R. Alley, et al., Climate change 2007: the physical science basis summary for policymakers, Paris, France, February 2007, Contribution of Working Group I to the Fourth Assessment Report of the Intergovernmental Panel on Climate Change (2007).
[3] Hamza Bennacer, et al., Indian J. Pure Appl. Phys. 53 (March) (2015) 181–189.
[4] V.L. Shaposhnikov, A.V. Krivosheeva, V.E. Borisenko, Phys. Rev. B85 (2012) 205201.
[5] A. Luque, J. Appl. Phys. 110 (2011), 00031301.
[6] R.H. Bube, Photovoltaic Materials, Imperial College Press, 1998, pp. 1–33.
[7] T. Ouahrani, A. Otero-de-la-Roza, R. Khenata, et al., Comp. Mater. Sci. 47 (2010) 655–659.
[8] F. Chiker, et al., Solid State Commun. 151 (2011) 1568–1573.
[9] J.L. Shay, J.H. Wernick, Ternary Chalcopyrite, Semiconductors: Growth, Electronic Properties and Applications, Pergamon Press, Oxford, Pergamon, New York, 1975.
[10] A. Continenza, S. Massida, A.J. Freeman, T.M.De. Pascale, F. Meloni, M. Serra, Phys. Rev. B 46 (1992) 10070.
[11] J.E. Jaffe, A. Zunger, Phys. Rev. B 27 (1983) 5176.
[12] A. Zunger, J.E. Jaffe, Phys. Rev. Lett. 51 (1983) 662.
[13] J.E. Jaffe, A. Zunger, Phys. Rev. B 29 (1984) 1882.
[14] J.E. Jaffe, A. Zunger, Phys. Rev. B 30 (1984) 741.
[15] A.G. Petukhov, W.R.L. Lambrecht, B. Segall, Phys. Rev. B 49 (1993) 4549.
[16] A.D. Martinez, A.N. Fioretti, E. Toberer, A.C. Tamboli, J. Mater. Chem. A 5 (2017) 11418–11435.
[17] A.D. Martinez, et al., Development Of $ZnSiP_2$ for Si-based tandem solar cells, IEEE J. Photovolt. 5 (January (1)) (2015).
[18] A.D. Martinez, et al., Energy Environ. Sci. 9 (2016) 1031–1041.
[19] A. Spring-Thorpe, B. Pamplin, J. Cryst. Growth 3 (1968) 313–316.
[20] J.L. Shay, B. Tell, E. Buehler, J.H. Wernick, Phys. Rev. Lett. 30 (20) (1973) 983–986.
[21] W. Clark, R. Stroud, J. Phys. C Solid State Phys. 6 (13) (1973) 2184–2190.
[22] V. Kumar, S.K. Tripathy, J. Alloys Compd. 582 (2014) 101–107.
[23] G.D. Holah, J. Phys. C5 (1972) 1893.
[24] S. Gorban, V.A. Gorynya, V.I. Lugovoi, N.P. Krasnolob, G.I. Salivon, I.I. Tychina, Phys. Status Solidi B 93 (2) (1979) 531–538.
[25] S. Shirakata, T. Shirakawa, J. Nakai, Il nuovo Cimento della Societa italiana de Fisica 2 (6) (1983) 2058–2063.
[26] S.A. Lopez-Rivera, H. Galindo, B. Fontal, M. Briceno, Phys. Rev. B 30 (1984) 7097–7104.
[27] H. Pena-Pedraza, S.A. Lopez-Rivera, J.M. Martin, J.M. Delgado, Ch. Power, Mater. Sci. Eng. B 177 (2012) 1465–1469.
[28] P. Hohenberg, W. Kohn, Phys. Rev. B 864 (1964) 136.
[29] L.J. Sham, W. Kohn, Phys. Rev. 145 (1965) 561.
[30] S.C. Erwin, I. Zutic, Nat. Mater. 3 (2004) 410–414.
[31] S. Sahin, Y.O. Ciftci, K. Colakoglu, N. Korozlu, J. Alloys Compd. 529 (2012) 1–7.
[32] S.N. Rashkeev, S. Limpijumnong, W.L. Lambrecht, Phys. Rev. B 59 (1999) 2737–2748.
[33] W.R.L. Lambrecht, S.N. Rashkeev, J. Phys. Chem. Solids 64 (2003) 1615–1619.
[34] Limpijumnong, Lambrecht, Segall, Phys. Rev. B 60 (May (11)) (1999).
[35] Y. Yang, Y. Zhang, Q. Gu, H. Zhang, X. Tao, J. Cryst. Growth 318 (2011) 721–724.
[36] W. Gehlhoff, A. Hoffmann, Physica B 404 (2009) 4942–4948.
[37] T.Y. Wang, R. Sivakumar, D.K. Rai, W.T. Hsu, C.W. Lan, J. Chin. Inst. Chem. Eng. 39 (2008) 385–387.
[38] J.C. Rife, R.N. Dexter, P.M. Bridenbaugh, B.W. Veal, Phys. Rev. B 16 (1977) 4491–4500.
[39] M.C. Ohmer, J. Appl. Phys. 87 (2000) 4640–4641.
[40] G.C. Bhar, P. Kumbhakar, J. Appl. Phys. 87 (2000) 4638–4639.
[41] D.W. Fischer, M.C. Ohmer, J. Appl. Phys. 81 (1997) 425–431.
[42] D.W. Fischer, M.C. Ohmer, P.C. Schunemann, T.M. Pollak, J. Appl. Phys. 77 (1995) 5942–5945.
[43] S. Shirakata, J. Appl. Phys. 85 (1999) 3294–3300.
[44] X. Jiang, M.S. Miao, W.R.L. Lambrecht, Phys. Rev. B 71 (1–12) (2005) 205212.
[45] X. Jiang, M.S. Miao, W.R.L. Lambrecht, Phys. Rev. B 73 (1–4) (2006) 193203.
[46] F. Chiker, B. Abbar, S. Bresson, B. Khelifa, C. Mathieu, A. Tadjer, J. Solid State Chem. 177 (2004) 3859–3867.
[47] P. Zapol, R. Pandey, M. Ohmer, J. Gale, J. Appl. Phys. 79 (1996) 671–675.
[48] S.K. Tripathy, V. Kumar, Mater. Sci. Eng. B 182 (2014) 52–58.
[49] H.J.F. Jansen, A.J. Freeman, Phys. Rev. B 30 (1984) 561.
[50] J.P. Perdew, Y. Wang, Phys. Rev. B 45 (1992) 13244.

[51] G.K.H. Madsen, P. Blaha, K. Schwarz, E. Sjostedt, L. Nordstroṁ, Phys. Rev. B 64 (2001) 64.
[52] K. Schwarz, P. Blaha, G.K.H. Madsen, Comp. Phys. Commun. 147 (2002) 147.
[53] P. Blaha, K. Schwarz, G.K.H. Madsen, D. Kvasnicka, J. Luitz, WIEN2K: An Augmented Plane Wave Plus Local Orbitals Program for Calculating Crystal Properties, Vienna University of Technology, Vienna, Austria, 2001, ISBN: 3- 9501 031-1-2.
[54] J.P. Perdew, Y. Wang, Phys. Rev. B 45 (1992) 13244.
[55] J.P. Perdew, A. Ruzsinszky, G.I. Csonka, O.A. Vydrov, G.E. Scuseria, L.A. Constantin, X. Zhou, K. Burke, Phys. Rev. Lett. 100 (2008) 136406.
[56] E. Engel, S.H. Vosko, Phys. Rev. B 47 (1993) 13164.
[57] F. Tran, P. Blaha, Phys. Rev. Lett. 102 (2009) 226401.
[58] D. Koller, F. Tran, P. Blaha, Phys. Rev. B 83 (2011) 195134.
[59] Tarik Ouahrani, Khenata Reshak, Amrani Baltache, Bouhemadou, Phys. Status Solidi B 1–7 (2010), http://dx.doi.org/10.1002/pssb.200945463.
[60] H. Jiang, J. Chem. Phys. 138 (2013) 134115.
[61] S.D. Guo, B.G. Liu, EPJ Photovolt. 93 (2011) 47006.
[62] S.W. Fan, L.J. Ding, Z.L. Wang, K.L. Yao, Appl. Phys. Lett. 102 (2013) e022405.
[63] B.G. Yalcin, Appl. Phys. A 122 (456) (2016) 1e17.
[64] S. Bagci, B.G. Yalcin, J. Phys. D Appl. Phys. 48 (2015) 475304.
[65] B.G. Yalcin, Physica B 462 (2015) 64e69.
[66] A.D. Becke, E.R. Johnson, J. Chem. Phys. 124 (2006) 221101.
[67] A.D. Becke, M.R. Roussel, Phys. Rev. A 39 (1989) 3761.
[68] M. Hadjab, et al., Mater. Chem. Phys. 182 (October (1)) (2016) 182–189.
[69] P.E. Blochl, O. Jepsen, O.K. Anderson, Phys. Rev. B 49 (1994) 16223.
[70] F. Annane, H. Meradji, S. Ghemid, F. El Haj Hassan, Comp. Mater. Sci. 50 (2010) 274–278.
[71] C. Ambrosch-Draxl, J.O. Sofo, Comput. Phys. Commun. 175 (2006) 1–14.
[72] R. Del Sole, R. Girlanda, Phys. Rev. B 48 (1993) 11789.
[73] F.D. Murnaghan, Proc. Natl. Acad. Sci. U. S. A. 30 (1944) 244–247.
[74] S.C. Abrahams, J.L. Bernstein, J. Chem. Phys. 52 (1970) 5607.
[75] R. Brian, Pamplin, et al., Prog. Cryst. Growth Charact. 1 (1979) 331–387.
[76] P. Deus, H. Schneider, Phys. Status Solidi A 79 (1983) 411.
[77] G.-Q. Yao, H.-S. Shen, R. Kershaw, K. Dwight, A. Wold, Mat. Res. Bull. 21 (1986) 6534660.
[78] S.R. Zhang, L.H. Xie, S.D. Ouyang, X.W. Chen, K.H. Song, Phys. Scr. 91 (2016) 015801.
[79] S. ullah, et al., Physica B 441 (2014) 94–99.
[80] Sadao Adachi, Properties of Group-IV, III –V and II –VI Semiconductors, John Wiley & Sons, Ltd, 2005, ISBN: 0-470-09032-4.
[81] B. Merabet, H. Abid, N. Sekkal, Physica B 406 (2011) 930–935.
[82] M.I. Ziane, et al., Mater. Sci. Semicond. Process. 30 (2015) 181–196.
[83] J.L. Martins, Alex Zunger, Phys. Rev. Lett. 53 (13) (1986) 1400–1403, 31 March.
[84] T. Maeda, et al., Jpn. J. Appl. Phys. 50 (2011) 04DP07.
[85] Richard Corkish, Sol. Cells 31 (1991) 537–548.
[86] M. Fox, Optical Properties of Solids, Oxford University Press, New York, 2001.
[87] S. Berrah, A. Boukortt, H. Abid, Physica E 41 (2009) 701.
[88] Sadao Adachi, Properties of Semiconductor Alloys: Group-IV, III–V and II–VI Semiconductors, John Wiley & Sons, Ltd, 2009, ISBN: 978-0-470-74369-0.
[89] M. Hadjab, et al., Optik 127 (2016) 9280–9294.
[90] unlabelleda D.E. Aspnes, A.A. Studna, Phys. Rev. B 27 (2) (1983);
unlabelledb A. Boukortt, S. Berrah, R. Hayn, A. Zaoui, Physica B 405 (2010) 763–769.
[91] Omkar Jani, Christiana Honsberg, Ali Asghar, et al., January 3–7, the 31st IEEE Photovoltaic Specialists Conference (2005).
[92] B. Amin, R. Khenata, A. Bouhemadou, et al., Physica B 407 (2012) 2588–2592.
[93] Anima Ghosh, R. Thangavel, M. Rajagopalan, J. Mater. Sci. 50 (2015) 1710–1717.
[94] S.R. Zhang, et al., Phys. Scr. 91 (2016) 015801.
[95] Dietz, et al., Appl. Phys. Lett. 65 (November (22)) (1994).
[96] M.A. Green, Sol. Energy Mater. Sol. Cells 92 (2008) 1305–1310.
[97] M.I. Ziane, et al., Optik 157 (2018) 248–258.
[98] H. Boudriot, et al., Phys. Status Sol. (b) 108 (K129) (1981).